ARTICLES

Pressure-driven channel flows of a model liquid-crystalline polymer

J. Feng[a] and L. G. Leal
Department of Chemical Engineering, University of California–Santa Barbara, Santa Barbara, California 93106-5080

(Received 31 August 1998; accepted 25 June 1999)

Shear flows disrupt molecular orientation in liquid-crystalline polymers (LCPs) through director tumbling, and this causes difficulty in controlling the polymer structure and properties in injection molding and extrusion. In this paper we simulate LCP channel flows using the Doi theory. A Bingham closure is used to preserve director tumbling and wagging. The objective is to examine how contractions and expansions in a channel affect LCP orientation and to explore the possibility of using the channel geometry as a means of manipulating LCP order. A finite-element method is used to solve the coupled equations for fluid flow and polymer configuration. Results show that a contraction aligns the director with the streamline and improves molecular order, while an expansion drives the director away from the flow direction and reduces molecular order. If the expansion is strong enough, an instability develops downstream as disturbances in the flow and polymer configuration reinforce each other through the polymer stress. This instability generates a wave that spans roughly the central half of the channel and propagates downstream at the centerline velocity. For abrupt contractions or expansions, disclinations of $\pm 1/2$ strength arise in the corner vortex. The numerical results agree qualitatively with experiments when comparisons can be made. In particular, the wavy pattern following a sudden expansion is remarkably similar to previous experimental observations. The simulations suggest that using contractions and expansions may be a feasible strategy for controlling LCP order and morphology in processing. [S1070-6631(99)02710-5]

I. INTRODUCTION

Since the invention of Kevlar™, liquid-crystalline polymers (LCPs) have been used mostly as fibers. Producing three-dimensional parts through injection molding or extrusion has been largely unsuccessful. The main problem is that such processes involve pressure-driven channel flows that are dominantly shear flows. Unlike extensional flows in fiber spinning, where the stretching aligns the LCP molecules to produce relatively uniform orientation, shear flows cause director tumbling that disrupts orientational order. The result is a proliferation of orientational defects known as disclinations, which eventually lead to a polydomain morphology of the polymer.[1] Since the molecular orientation cannot be controlled during processing, the finished product is often plagued with nonuniformity, anisotropy, and weldlines. The key to solving such problems is an understanding of the relationship between the material structure and the flow. Thus, fluid mechanics plays a central part in the processing of microstructured materials.

Owing in part to their practical importance, channel flows of LCPs have received considerable attention in the past. Experimental studies, mainly using lyotropic HPC and PBG solutions, have discovered a host of intriguing phenomena peculiar to LCPs. In a straight channel, an anomalous velocity maximum occurs near the sidewalls at low flow rates[2] but disappears at higher flow rates.[3,4] Baleo and Navard[5] and Bedford *et al.*[4,6] documented the effects of varying the cross-sectional area of a channel on the LCP orientational order and the flow field. In particular, a large-scale wavy pattern appears downstream of an expansion. This pattern is believed to result from an instability related to upstream director orientations that are twisted away from the flow direction by the expansion. Similar patterns also occur for thermotropic LCPs in injection molding and extrusion (see Fig. 1 of Ref. 6). Kawaguchi and Denn[7] observed complex three-dimensional flow patterns in a conical contraction of the thermotropic Vectra A.

Theoretical understanding of LCP channel flows has lagged behind experimental explorations. This is not unique to channel flows but is generally true for LCP flows. The main obstacle is the lack of an appropriate theoretical model for the LCP rheology in the regimes of interest. Three rheological models have been used widely: the Leslie–Ericksen theory, a continuum theory based on the Landau–de Gennes free energy expansion, and the Doi theory. None gives an adequate description of complex LCP flows.

[a]Current address: The Levich Institute and Department of Mechanical Engineering, Steinman Hall #1M, City College of CUNY, 140th Street and Convent Avenue, New York, NY 10031.

The Leslie–Ericksen theory applies to slow flows in which the molecular orientation distribution is not perturbed from its equilibrium state. Its predictions for weak shear flows, e.g., the roll-cell instability, generally agree with observations.[8] A phenomenological extension of the theory to polydomains gives the correct scaling for the region II dynamics.[9] However, the Leslie–Ericksen theory is not applicable to processing flows of LCPs which typically are strong enough to distort the molecular orientation distribution. These flows correspond to the Deborah number cascade and region III of the viscosity curve.[1] In an attempt to describe changes in the molecular orientation distribution, a continuum theory was formulated by postulating a free energy in the form of the Landau–de Gennes expansion.[10–12] This approach has been criticized because the expansion is valid only in the neighborhood of the isotropic state[13] and does not converge for the moderately high order parameters typical of real LCP systems.[14] As possible symptoms of the fault, the theory predicts maxima in the shear and normal stresses[10] and fails to produce the second change of sign in the normal stress at high flow rates that has been experimentally documented.[15] Greco[16] also criticized the phenomenological nature of the theory. The unknown coefficients in the expansion have to be fitted to the isotropic state of the material, and once fixed, they cannot reflect the changes in the material effected by flow. This is a particularly serious flaw if one hopes to describe flow-induced complex structures such as disclinations. The Doi theory[17,18] differs from the above theories in that it is a molecular theory. It models a LCP as an ensemble of thin rigid rods that rotate as a result of Brownian motion, viscous torque, and intermolecular forces. Though this may not be a precise description of any real LCP system, it is a physically realizable nematic fluid and serves as a *model LCP* whose dynamic behavior can be meaningfully compared with experiments. So far, such comparisons have been done only for the simplest flows and the results are encouraging. For example, the theory gives qualitatively and sometimes quantitatively accurate predictions of the shear rheology of certain lyotropic LCPs.[19,20] It has also been argued that a molecularly based theory is advantageous in describing the severe distortion in orientation near disclinations.[16,21] Therefore, the Doi theory appears to be the most promising model for complex LCP flow simulations.

Unfortunately, the Doi theory has a shortcoming that hampers its application to flow simulations: it does not contain distortional elasticity, i.e., elasticity due to spatial variation of the LCP configuration. Although for certain inhomogeneous flows the theory permits disclinations and multiple domains as solutions,[22] in the absence of distortional elasticity it is unable to predict the *proliferation* of disclinations and the polydomain structure in real LCPs. The consequence of this is well illustrated by previous attempts to use the theory for flow calculations. In a simple shear, the Doi theory predicts director tumbling in certain parameter ranges, while the flow of a real LCP always appears steady. Marrucci and Maffettone[23] and Larson[19] *assumed* a polydomain structure with the tumbling of each domain determined by the Doi theory. Then by averaging over the domains, they obtained steady results that can be compared with experiments. Such an averaging scheme fails for complex flows, however, because the orientational distribution of the domains (or equivalently, the phase difference between domains) is *a priori* unknown. Alternatively, a quadratic closure approximation has been used to artificially suppress director tumbling in shear-dominated flows.[24–26] This treatment is unsatisfactory since it attempts to mend one failing of the Doi theory—the lack of distortional elasticity—by introducing another, namely the loss of director tumbling in shear flows due to the quadratic closure. Hence, a realistic simulation of LCP channel flows has to contain two essential elements: director tumbling and distortional elasticity. Director tumbling is already in the Doi theory; it simply needs to be brought out by a more sensible closure approximation (or by solving for the orientation distribution with no closure). Distortional elasticity has been added to the Doi theory through a nonlocal nematic potential.[21,27] However, the resulting model is complex and solutions have been obtained only in static situations, where the effects of the distortional elasticity on disclinations has been explored.[16,28] No flow calculation has been done so far.

In the present paper we take a different path by simulating LCP channel flows using the original Doi theory. Distortional elasticity is not included but director tumbling and wagging are preserved by using a Bingham closure.[29] In other words, we simulate channel flows of a *model LCP* with negligible distortional elasticity. The rationale for such an approach is twofold. First, director tumbling is one of the two major factors in such simulations, and has been excluded in previous studies on channel flows.[24–26] By including director tumbling but not distortional elasticity, we are in a sense solving half of the problem. In view of the complexity of the new model, this is a sensible approach at this stage and it complements studies of the distortional elasticity in the absence of flow.[28] The present results will serve as a benchmark against which the effects of distortional elasticity will be assessed in channel flows. Second, these numerical results may be directly relevant to the flow of a real LCP. Such relevance may be restricted to certain areas of the flow where distortion of the orientation field is mild or it may be restricted to certain properties of the LCP that are insensitive to the distortional elasticity. Indeed, the numerical results will be seen to qualitatively agree with experiments where comparisons can be made.

Corresponding to the twofold rationale for this study, we hope to achieve two objectives. The first is to gain physical insights into the coupling between flow and polymer orientation that will help us understand the ''complete solution'' when distortional elasticity is added. The second objective is more concrete and practical. We wish to demonstrate how contractions and expansions in an otherwise straight channel affect the motion of the director and the degree of order. In homogeneous flows, director tumbling may be suppressed by a minute amount of extensional flow.[30,31] Channel flow experiments indicate that contractions enhance the degree of order, presumably by aligning either individual molecules or domains.[4,5] We will test the feasibility of using contractions and expansions as a strategy for controlling LCP orientational order in flows that are relevant to extrusion and injec-

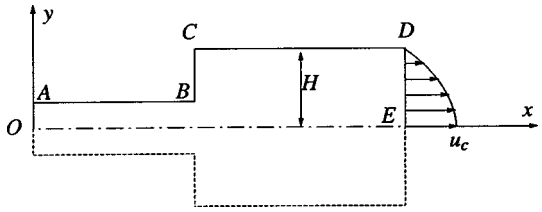

FIG. 1. Schematic of a channel flow geometry. The computational domain consists of the upper half because of symmetry. H is the half-width of the wider part of the channel, and u_c is a *nominal* centerline velocity at the inlet or outlet, whichever is wider, evaluated for a Stokes flow driven by the same pressure drop. $\Gamma = u_c/H$ is the characteristic strain rate used in defining the Peclet number of the flow.

tion molding. Another outstanding question is the peculiar wave pattern observed downstream of expansions. We will seek an explanation for the apparent instability in the coupling between fluid flow and polymer dynamics.

The rest of the paper is organized as follows. Section II describes the theoretical model and sets up the numerical problem. Section III presents numerical results for a straight channel as a validation of the numerical scheme and a prerequisite for later discussions. Section IV deals with channels with gradual and abrupt contractions, and Sec. V studies channels with gradual and abrupt expansions. Finally in Sec. VI we summarize the results and discuss their implications for LCP processing.

II. FORMULATION OF THE PROBLEM

A. Governing equations

The Doi theory is a statistical-mechanical theory describing the orientation of an ensemble of rod-like LCP molecules suspended in a Newtonian solvent.[17,18] The theory is based on the orientation distribution function $\Psi(\mathbf{u})$, $\mathbf{u}$ being the unit vector along each rod. All rods have the same length L, and the number of polymers per unit volume is ν. Following the Prager procedure, the evolution equation of the second moment tensor $\mathbf{A} = \int \mathbf{uu}\Psi(\mathbf{u})d\mathbf{u} = \langle \mathbf{uu} \rangle$ can be derived:

$$\frac{\partial \mathbf{A}}{\partial t} + \mathbf{v}\cdot\nabla\mathbf{A} - \nabla\mathbf{v}^T\cdot\mathbf{A} - \mathbf{A}\cdot\nabla\mathbf{v} = -\frac{f}{\mathrm{Pe}}\left(\mathbf{A} - \frac{\delta}{3}\right) + \frac{fU}{\mathrm{Pe}}(\mathbf{A}\cdot\mathbf{A} - \mathbf{A}:\langle\mathbf{uuuu}\rangle) - 2\mathbf{D}:\langle\mathbf{uuuu}\rangle, \tag{1}$$

where δ is the unit tensor, $\mathbf{v}$ is the fluid velocity, and $\mathbf{D} = (\nabla\mathbf{v} + \nabla\mathbf{v}^T)/2$. The Peclet number is defined as $\mathrm{Pe} = \Gamma/(6D_r)$, where $\Gamma = u_c/H$ is the characteristic strain rate (see Fig. 1) and D_r is the rotational diffusivity in an isotropic solution of the same volume concentration. U is the nematic strength in the Maier–Saupe potential and f represents the tube dilation effect:[17]

$$f = (1 - S^2)^{-2} = \tfrac{4}{9}(1 - \mathbf{A}:\mathbf{A})^{-2}, \tag{2}$$

where $S = [(3\mathbf{A}:\mathbf{A} - 1)/2]^{1/2}$ is the order parameter.

The polymer stress may be written as

$$\tau = \left(\mathbf{A} - \frac{\delta}{3}\right) - U(\mathbf{A}\cdot\mathbf{A} - \mathbf{A}:\langle\mathbf{uuuu}\rangle) + \frac{\beta\mathrm{Pe}}{(\nu L^3)^2}\mathbf{D}:\langle\mathbf{uuuu}\rangle, \tag{3}$$

where τ has been scaled by $3\nu kT$, k being the Boltzmann constant and T the temperature. $(\nu L^3)^2$ is the crowdedness factor and $\beta = O(10^3)$ is an empirical parameter. This stress enters the equations of motion for the fluid:

$$\mathrm{Re}\frac{\partial \mathbf{v}}{\partial t} = -\nabla p + \nabla^2\mathbf{v} + \frac{c}{\mathrm{Pe}}\nabla\cdot\tau, \quad \nabla\cdot\mathbf{v} = 0, \tag{4}$$

where the Reynolds number is defined as $\mathrm{Re} = \rho u_c H/\mu_s$, with ρ and μ_s being the density of the fluid and the constant solvent viscosity, respectively. $c = \nu kT/(2\mu_s D_r)$ is the concentration parameter. The inertia of LCP flows is typically small; the $\partial\mathbf{v}/\partial t$ term is kept to give a sense of the transient of the flow. It is in fact insignificant since Re is small.

Hence, complex flows of LCPs are determined by the polymer stress, which in turn depends on polymer configuration, which itself is determined by the flow. However, the theory as represented by Eqs. (1)–(4) is not self-contained because of the fourth moment tensor $\langle\mathbf{uuuu}\rangle$. In order to ''close'' the theory at the level of the second moment tensor $\mathbf{A} = \langle\mathbf{uu}\rangle$, $\langle\mathbf{uuuu}\rangle$ needs to be expressed in terms of $\mathbf{A}$ via a closure approximation. In this paper we use the so-called Bingham closure, which is based on postulating a special form for the orientation distribution function.[29,32] It is exact in the weak flow limit and predicts the correct equilibrium properties such as the isotropic–nematic transition. In simple shear, it preserves director wagging and tumbling. The only significant limitation of the Bingham closure, vis-à-vis the unapproximated Doi model, is that it does not predict the transition from wagging to flow aligning in simple shear at high Peclet number, but instead substitutes a monotonic decrease in the amplitude of wagging as Pe increases. For most purposes, the distinction between flow-aligning and small-amplitude wagging will not be important. As far as we know, all previous simulations of complex LCP flows used the quadratic closure.[24,25] That closure suppresses director tumbling in shear which is an essential feature of channel flows. Finally, inhomogeneous flow calculations have shown the Bingham closure to be the best among all popular second-order closures.[31]

The Doi theory applies to rigid-rod LCPs, lyotropics (solutions) and thermotropics (melts) alike. Since lyotropic LCPs are usually more rigid than thermotropics, the Doi theory is thought to be more pertinent to solutions, though the tube model does not discriminate between melts and solutions.[18] For melts, the only difference is that there is no viscous stress either from the solvent directly or from the friction on LCP molecules. In this paper, we will compare the numerical results with experiments done with lyotropics.

B. Boundary conditions

Once the time-dependent nature of LCP dynamics is preserved, the channel flow becomes a uniquely difficult prob-

lem because of velocity boundary conditions at the inlet and outlet. For the channel flow of a Newtonian fluid, it is customary to specify a fully developed velocity profile at the inlet and use the so-called traction-free boundary condition at the outlet. The latter is conveniently treated as a natural boundary condition in finite-element algorithms. For a viscoelastic fluid with deviatoric stress τ, the traction-free condition does not hold in general because the normal stress difference varies across the channel at the exit.[33] When the finite-element weak form is written using a test function $\mathbf{w}$, there will be a surface integral term

$$\int_{\partial\Omega}[-p\mathbf{n}+\mathbf{n}\cdot(\mu_s\nabla\mathbf{v}+\tau)]\cdot\mathbf{w}d\Gamma \tag{5}$$

that needs to be computed along the portion of the boundary where the velocity is not specified. To avoid this trouble, a fully developed velocity profile is always used on the inlet and outlet of channel flows; see, e.g., Purnode and Crochet[34] for a FENE-P fluid and Armstrong *et al.*[24] for a nontumbling LCP.

Because of the inherently periodic dynamics of LCPs, the very concept of a ''fully developed flow'' needs to be examined. Picture the flow in a long straight channel in which there is no variation along the flow direction. The director will tumble, wag, or align depending on the lateral position, and this modifies the flow. As will be seen in Sec. III A, no steady state will be achieved that may serve as a fully developed profile. Alternatively, one could fix the inlet velocity profile and polymer configuration, and let the two evolve in a long entry section. This will lead to a spatially varying solution. Since the variations along a streamline never die out, again no fully developed profile appears downstream. To sum up, it is unreasonable to specify Dirichlet velocity profiles at the inlet or outlet for channel flows of our model LCP. Instead, we need to use Neumann conditions and evaluate the surface integral of Eq. (5).

We require $\partial u/\partial x=0$ and $v=0$ at the inlet and outlet of a channel flow (i.e., *OA* and *DE* in Fig. 1). Then pressures profiles $p_{\text{in}}(y)$ and $p_{\text{out}}(y)$ need to be specified on *OA* and *DE* by applying momentum conservation along the tangential direction on the boundary.[35] The pressure values on the centerline p_E and p_O are given at the outset and the pressure profiles are computed each time step. The weak form of Eq. (4) is

$$\begin{aligned}\text{Re}\int_\Omega\frac{\partial\mathbf{v}}{\partial t}\cdot\mathbf{w}d\Omega=&\int_\Omega\left[p\nabla\cdot\mathbf{w}-\nabla\mathbf{v}:\nabla\mathbf{w}-\frac{c}{\text{Pe}}\tau:\nabla\mathbf{w}\right]d\Omega\\&+\int_{\partial\Omega}\mathbf{n}\cdot\left[-p\mathbf{w}+\nabla\mathbf{v}\cdot\mathbf{w}+\frac{c}{\text{Pe}}\tau\cdot\mathbf{w}\right]d\Gamma,\end{aligned} \tag{6}$$

where the test function $\mathbf{w}$ is also the shape function in our Galerkin formulation. The last term is the surface traction that needs to be evaluated at *OA* and *DE* for the x component of the flow. The y component has Dirichlet boundary condition $v=0$ at all boundary segments.

To summarize, we use the following boundary conditions in the channel flow simulations (cf. Fig. 1):

ABCD (solid wall):	$u=0,\ v=0$
OE (centerline):	$\partial u/\partial y=0,\ v=0$
OA (inlet):	$\partial u/\partial x=0,\ v=0,\ p=p_{\text{in}}(y),\ \partial\mathbf{A}/\partial x=0$
DE (outlet):	$\partial u/\partial x=0,\ v=0,\ p=p_{\text{out}}(y).$

For Newtonian fluids, Pironneau has shown this formulation to be well-posed.[36] Because of the hyperbolic nature of Eq. (1), an inlet condition is necessary for $\mathbf{A}$ and we impose a homogeneous Neumann condition. Downstream, $\mathbf{A}$ evolves along the characteristics which are streamlines. Initially there is no flow in the channel and the LCP is at its equilibrium order with a uniform director field. Then a pressure drop specified by p_O and p_E is suddenly applied and the flow starts. We use a finite-element method to solve the coupled Eqs. (1), (3), and (4). The numerical scheme differs from that of Feng and Leal[22] only in that the surface traction term is added here to drive the flow [see Eq. (6)]. A triangular mesh is used and mesh refinement has been done routinely to ensure convergence of the results. To avoid stress singularity, the corner *B* is rounded in some of the simulations.

C. Parameter values

The following parameter values are used: $\beta=1000$, $\text{Re}=10^{-2}$, $(\nu L^3)^2=2\times10^6$, $c=100$, $U=8$, and $\text{Pe}=40$. The small Reynolds number ensures a short initial transient of the fluid flow after the startup. The crowdedness factor is typical of lyotropic systems used in experiments. It is not clear what c values are representative of real LCPs. Doraiswamy and Metzner[37] and Mori *et al.*[25] fitted the approximate Doi theory based upon the quadratic closure to measured values of the steady shear viscosity for LCP solutions. However, this procedure is problematic. The model produces a steady-state shear viscosity because the quadratic closure artificially suppresses director tumbling. In the experiment, however, the steady state is a manifestation of the polydomain structure, perhaps with each domain tumbling continuously. Here we use a moderate c so that the flow and polymer dynamics are coupled yet the polymer stress does not distort the flow kinematics beyond recognition. The U and Pe values are chosen based on the solution diagrams for the Bingham closure.[31] The closure does not allow steady alignment beyond a certain U, and a small U would therefore be needed to simulate director alignment at the wall. Then tumbling would be confined to a narrow strip at the center of the channel. Since in this work we are more interested in director tumbling than alignment, the current values of U and Pe are chosen such that the director tumbles in the central part of the channel and wags near the wall.

D. Simplifications

We assume that the flow field is two-dimensional in the $x-y$ plane and the director orientation is symmetric with respect to that plane. This symmetry assumption excludes director kayaking from this work. Kayaking is a rather exceptional regime of director motion[38] and its inclusion would make the flow three-dimensional and much more costly to compute. Now the configuration tensor $\mathbf{A}$ has three unknown components:

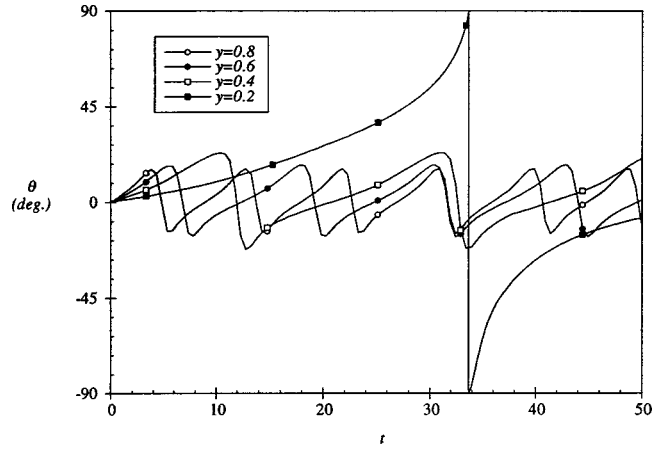

FIG. 2. Motion of the director at different y in a straight channel. The centerline is at $y=0$ and the solid wall at $y=1$. Wagging prevails in the upper part of the channel and gives way to tumbling closer to the centerline at $y\approx 0.2$.

$$\mathbf{A}=\begin{bmatrix} A_1 & A_2 & 0 \\ A_2 & A_3 & 0 \\ 0 & 0 & 1-A_1-A_3 \end{bmatrix} \tag{7}$$

and may be graphically represented by an ellipsoid. The longest axis is along the director, and the relative magnitude of the axes indicates the degree of orientational order.

Considering the above assumptions and the lack of distortional elasticity in the Doi theory, one should be cautious in interpreting the numerical results. The simulations nonetheless bear on real LCP flows in two ways. First, the physical mechanisms that the simulations reveal, for instance the coupling between director tumbling and flow, operate in the real flow, albeit moderated perhaps by distortional elasticity or out-of-plane orientations. Second, the results may apply more directly in certain cases. Strong orientational distortion may be restricted to certain regions of the flow such as wall layers and domain boundaries. And then in other regions the predictions will be directly applicable. Comparisons with experiments indeed seem to vindicate such expectations.

III. PLANAR POISEUILLE FLOW

A simulation of the flow in a straight channel (or a Poiseuille flow) serves two purposes. First, it validates the numerical scheme, especially the formulation of the surface traction as the driving force of the flow. Though inhomogeneous in the transverse direction, the flow is everywhere shear and the simulation can be compared with known behavior of the LCP in simple shear flow. For this reason, we have computed the Poiseuille flow using a two-dimensional mesh although the problem itself is one-dimensional. Second, the straight channel simulation serves as a base line for studying more complex channel flows in the following sections.

Initially the director is uniformly aligned with the x axis. After the pressure gradient is applied, a Newtonian velocity field quickly develops. The relaxation time of the LCP is much longer, and as the polymer configuration evolves the flow field deviates from the Newtonian one. For the nematic

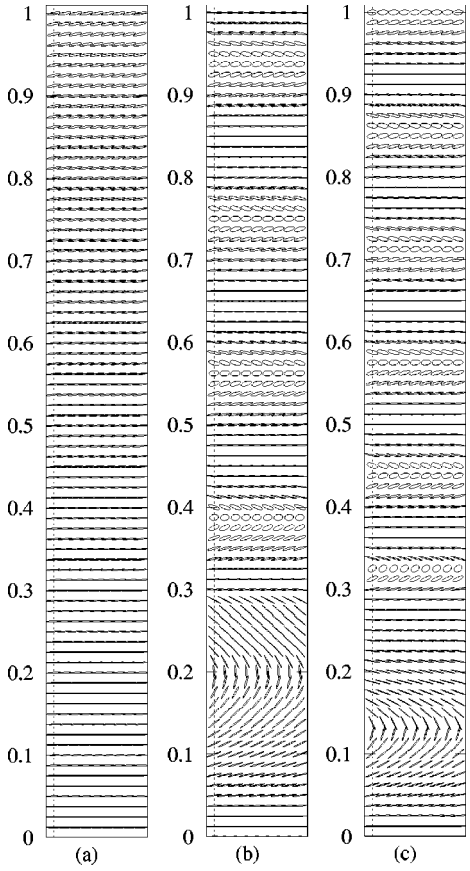

FIG. 3. Snapshots of the **A** field at different times: (a) $t=2.5$—the director turns toward the axis of compression of the flow; (b) $t=34$—the first tumbling wave emerges above $y=0.2$; (c) $t=46$—the waves accumulate and their spacing narrows.

strength $U=8$ and the nominal Peclet number (defined using the characteristic strain-rate u_c/H; see Fig. 1) $\mathrm{Pe}=40$, the shear rate at the wall corresponds to director wagging. As the shear-rate decreases toward the centerline, the wagging amplitude increases and the frequency decreases until wagging becomes tumbling. Figure 2 shows that this transition occurs somewhere between $y=0.2$ and 0.4, in agreement with estimation based on the solution diagram of the Bingham closure[31] and a parabolic velocity profile.

The configuration tensor **A** can be graphically represented by an ellipsoid, with its major axis along the director and its shape indicating the order parameter. Figure 3 shows snapshots of the **A** field as represented by projection of the ellipsoids on the flow plane. The ellipsoids are not axisymmetric in general and their third axis cannot be shown here. As in a simple shear flow,[19] the local order parameter decreases when the director is along the axis of compression of the shear and the ellipse becomes plumper. Since the frequency of wagging and tumbling scales with the local shear rate, the director rotation occurs sooner on one streamline than on the next inside. This gives rise to ''wave fronts'' of plump ellipses propagating toward the centerline. No matter is transported across the stream, of course, and there is no interference between neighboring streamlines in terms of the director motion. As the flow continues, more and more strips are generated and their spacing becomes narrower. As a strip

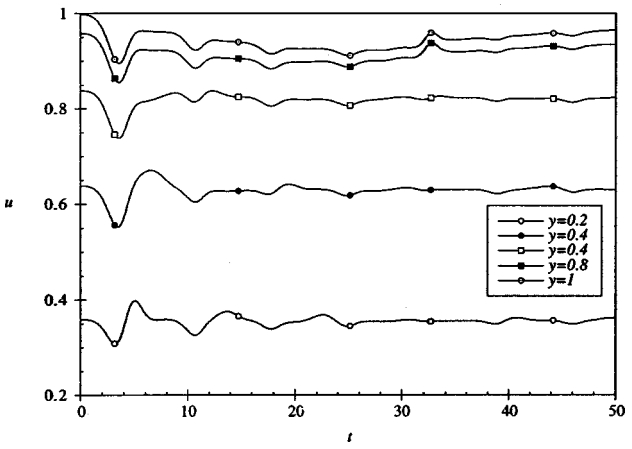

FIG. 4. Variation of the velocity component u at different y in the straight channel. The oscillations are caused by director wagging and tumbling.

approaches the centerline the ''wave speed'' decreases and it will never reach the centerline. Because the tumbling and wagging period varies continuously with y, the entire flow field is aperiodic. No steady state will be achieved.

Figure 4 shows the variation of velocity as a consequence of the director motion. Initially there appears to be concerted flow reduction and subsequent recovery across the channel. Later the undulation becomes less prominent. The key to understanding the flow modification is the polymer shear stress τ_{xy}, which has three contributions from the Brownian, nematic, and viscous terms of Eq. (3), each depending on the polymer configuration. The nematic part oscillates in phase with θ and the Brownian part out of phase with θ. The viscous part behaves precisely as in a suspension of rods and is much smaller than the other two. So the total stress is determined by the competing nematic and Brownian contributions and the former is larger. Hence, the total shear stress is roughly in phase with θ. When the director is along the compression axis of the flow ($\theta>0$), the polymer contributes a positive shear stress to the flow and effectively the fluid viscosity is increased. When the director is stretched ($\theta<0$), the polymer contributes a negative shear stress to the flow and the viscosity is effectively reduced. Since the nematic term contributes the most to the total stress, the behavior of the LCP solution, e.g., the viscosity reduction, cannot be intuitively inferred from that of a suspension of rods.

After the flow starts, the director first rotates into the compression axis of the flow throughout the channel [Fig. 3(a)]. This increases the effective shear viscosity in the channel. Since the pressure gradient along x is fixed, the flow rate drops across the channel as seen in Fig. 4. Later as the first wagging wave propagates away from the wall toward the centerline, a layer of ''effectively thinned'' fluid trails behind, causing the recovery of the velocity. As more waves appear, the ''thinned'' and ''thickened'' layers tend to cancel each other and the fluctuation in velocity dies out in amplitude. The unusual peaks near the centerline at $t=34$ reflect the birth of the low-viscosity layer behind the first tumbling wave [cf. Fig. 3(b)]. Afterwards the high-viscosity layer above the centerline narrows as the tumbling wave front progresses, yielding the gradual increase in u near the centerline. Because of the unsteady director motion, no steady ''fully developed velocity profile'' will obtain in the channel.

The pattern in Fig. 3 can be seen as a one-dimensional polydomain structure, although in the absence of distortional viscosity, the ''domain size'' shrinks indefinitely. The pattern also resembles the wind-up picture in simple shear.[39] In a real flow, as the spatial gradient of polymer configuration grows, distortional elasticity would drive the director out of the flow plane and generate three-dimensional roll cells and eventually disclinations.[1] Such processes cannot be represented in our simulations since we assume a two-dimensional flow and negligible distortional elasticity. The simulation also differs from reality in the near-wall region. Since closure models based on the second moment tensor $\mathbf{A}$ generally fail to predict flow-aligning in simple shear,[31] we could not predict steady alignment at the wall. With distortional elasticity added, wall anchoring should help remove this difficulty. With that caveat, the wagging region next to the wall can be related to the well-aligned wall layer observed in experiments (zone I in Fig. 2 of Baleo and Navard,[5] see also Ref. 40). The tumbling region close to the centerline is readily identified with zone II of Ref. 5 in which director tumbling prevails and the birefringence is low.

IV. CONTRACTIONS

We have simulated channel flows with a single gradual or abrupt contraction, or a single gradual or abrupt expansion. In all four cases, the characteristic strain rate (cf. Fig. 1) is held fixed at a value which corresponds to $\mathrm{Pe}=40$. Initially the director is uniformly aligned in the horizontal direction and the order parameter is at the equilibrium value. There is no flow in the channel and a pressure drop is suddenly applied between the inlet and the outlet at $t=0$. The initial condition on the director field affects the phase of wagging and tumbling but not the main features of the solution.

The qualitative effects of converging and diverging flows on director orientation are, in some respects, easy to anticipate. Specifically, we expect a converging flow to induce alignment in the flow direction and increase the orientational order. In contrast, a diverging flow will tend to induce alignment perpendicular to the flow direction, and in the process decrease the degree of orientational order. We shall see that our results conform to these expectations. Our emphasis, however, is on how the flow kinematics affects director tumbling. We have already noted that a motivation for the present study of converging and diverging channels is the potential of introducing such modifications into the geometry of injection molds in order to suppress director tumbling and thus reduce disclination density in molded parts. For this potential application, the details of director dynamics cannot be ignored. For example, a contraction is useful only if the alignment produced propagates far enough downstream and is relatively uniform across the channel. In many cases, it would be necessary to follow a contraction with an expansion or vice versa, and so the efficacy of modifying the mold geometry would depend on the combined effect of both.

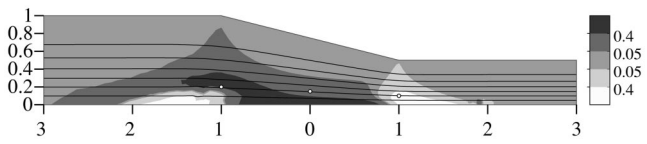

FIG. 5. Streamlines (curves) and contours of the flow-type parameter (gray-scale shading) in a channel with a 1:0.5 gradual contraction. The inlet of the channel is at $x=-3$ and the outlet is at $x=10$. The three open circles indicate spatial points (i)–(ii) at which the velocity is analyzed in Fig. 6.

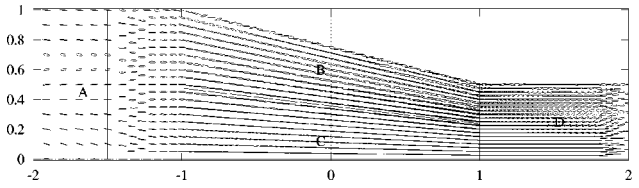

FIG. 7. The **A** field in the 1:0.5 gradual contraction at $t=50$. The solid straight lines delineate four regions A–D based on the local polymer dynamics.

A. Gradual contractions

We begin by considering a 1:0.5 gradual contraction over an axial distance of 2. Figure 5 shows the streamlines and the flow type parameter[41] in the channel at $t=0.05$. At this time the kinematics of the flow has developed but the LCP configuration has hardly responded to the flow. For the parameters used, flow modification is mild throughout the simulation and the qualitative characteristics of the flow field are unaltered by the polymer stress. The contraction causes an extensional flow region, as expected, but this extends from the centerline to only about one-half of the channel width. In the part of the channel closer to the walls, the flow is mostly shear, even within the contraction zone, and there is only a weak extensional component superposed on this base flow. Finally, upstream and downstream of the contraction, there are two small rotational areas near the centerline. Although these appear in Fig. 5 to include the centerline, this is clearly an artifact due to the finite mesh size since rotation on the centerline is nil because of symmetry.

Figure 6 shows the temporal variation of the horizontal velocity component at three points in the contraction. These curves resemble Fig. 4 for a straight channel. The initial oscillation is well defined and represents fluctuations in the overall flow rate due to director wagging near the wall. Later, multiple frequencies set in because of wagging and tumbling at various locations throughout the channel.

Figure 7 illustrates the behavior of the LCP corresponding to the kinematics of Fig. 5. We divide the channel into four areas with distinct features of the polymer dynamics,

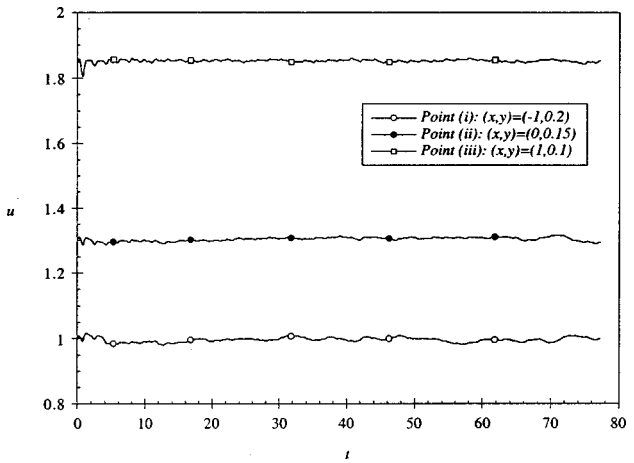

FIG. 6. Variation of the velocity component u at points (i)–(iii) in the 1:0.5 gradual contraction. The points are indicated by the three circles in Fig. 5 that fall roughly on a streamline.

and these are roughly delineated in the plot by solid lines. In area A, which is upstream of the contraction, the polymer does not ''feel'' the imminent contraction except through flow modification, which is small, and the LCP behavior is essentially the same as in a straight channel (cf. Sec. III). At the Peclet number $\mathrm{Pe}=40$ considered here, director tumbling occurs from the centerline up to $y\approx 0.2$ and wagging from there to the walls. Inside the contraction, the flow in region B nearest the walls is approximately simple shear with a shear rate that increases in the flow direction. Thus, it is no surprise that the director simply continues to wag about the flow direction with an increasing frequency and slightly decreased amplitude as we move downstream. This gives rise to spatial variations of director orientation along a streamline. We may note, however, that the prediction of wagging over the whole of region B is likely an artifact of the Bingham closure. As discussed earlier, the Doi model with the Bingham closure predicts wagging of decreasing amplitude in simple shear flow as the Peclet number is increased, rather than the transition to flow aligning that is predicted by the *exact* Doi model. We may thus anticipate that an exact solution of the Doi model for this flow would show the near-wall portion of region B to be flow aligning, rather than exhibiting small amplitude wagging. The weak extensional component of the flow in area B would enhance the tendency toward alignment in the flow direction.

It is in the region close to the centerline within the contraction, denoted as area C, that the effect of contraction is felt most strongly. Here, the flow is primarily extensional. Hence, as anticipated qualitatively, the director tumbling and wagging which appears near the centerline in the upstream area A is suppressed. The result is a director field that is highly aligned in the flow direction toward the end of Area C. It is noteworthy that the small rotational flow area at $x=-1.5$ does not have any noticeable downstream effect on the suppression of director tumbling. For the particular combination of Pe and U used in this case, the 1:0.5 gradual contraction is sufficient to suppress tumbling at all cross-channel positions. In any ''designed'' use of a contraction within a mold, an important parameter would be the minimum contraction ratio to suppress tumbling at all point across channel. Of course, this would depend not only on Pe and U, but also on the geometry of the contraction.

Downstream of the contraction, in the region denoted as area D, the flow returns to simple shear, and director tumbling must ultimately resume near the channel centerline, albeit in a thinner section than in area A since the average shear rate in D is higher. However, because the convection is

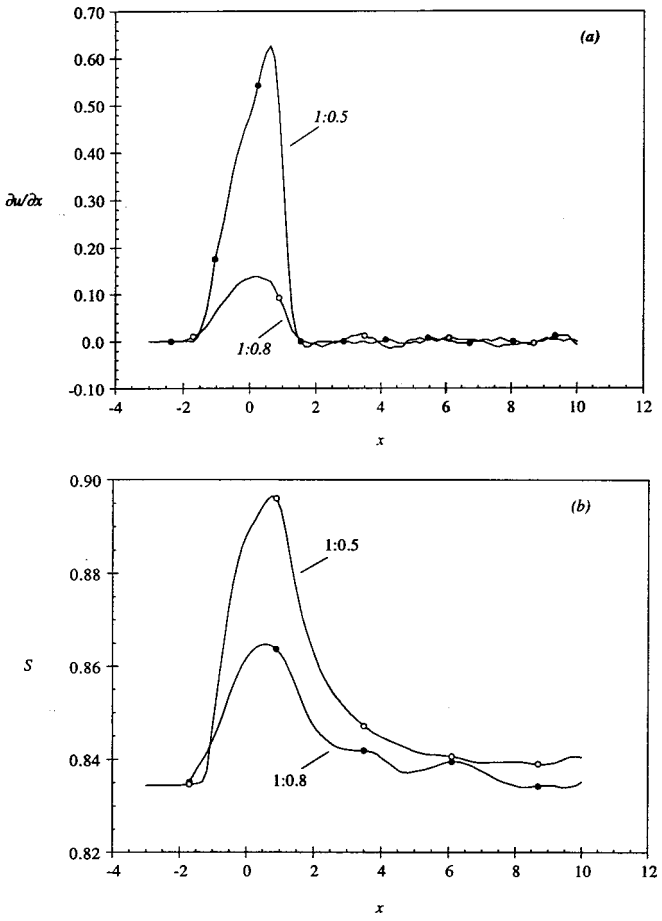

FIG. 8. Effects of the contraction ratio: comparison between the 1:0.8 and 1:0.5 gradual contractions. $t=50$. (a) The extension rate $\partial u/\partial x$ on the centerline; (b) the order parameter S on the centerline. The contraction is between $x=-1$ and $x=1$.

fast close to the centerline, the aligned state appears to persist for a considerable distance downstream before the effect of tumbling reappears. It may be noted, however, that the order parameter S starts to relax almost immediately after the fluid enters the narrow channel [see Fig. 8(b)]. This is in interesting contrast to the visual persistence of the uniform state into area D in Fig. 7. Clearly, the degree of alignment relaxes faster than the orientation of the director.

To quantify the effect of contractions, we have also computed a milder 1:0.8 gradual contraction over an axial distance of 2. As compared with the 1:0.5 contraction in Fig. 7, the area C in which flow aligning prevails is thinner, though tumbling is still suppressed across the whole channel. Also, the relatively uniform state does not extend as far into area D, partly because the centerline velocity is lower. Figure 8 compares the extension rate and order parameter along the centerline of the two contractions. The stronger contraction generates a maximum extension rate (near $x=0$) about four times that of the weaker contraction. This, not surprisingly, causes a stronger increase in the order parameter.

The qualitative features of these numerical simulations agree well with experiments. Baleo and Navard[5] and Bedford and Burghard[4] observed that contractions enhance streamwise alignment and molecular order, and the uniform state

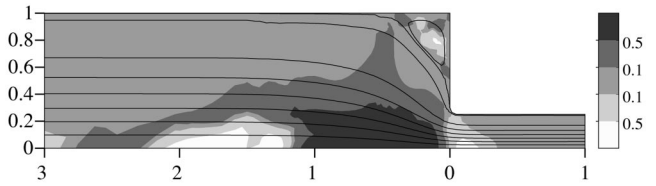

FIG. 9. Streamlines and contours of the flow-type parameter (gray-scale shading) in a channel with a 1:0.25 abrupt contraction. $t=34$. The flow is rotational in the center of the vortex. The corner at the lip of the contraction has been rounded to avoid stress singularity. The contraction is at $x=0$. The inlet is at $x=-3$ and outlet is at $x=3$.

persists downstream for a considerable distance. Furthermore, the profiles of extension rate and order parameter in Fig. 8 are very similar to the measurements of Bedford and Burghardt, though these authors believed that the increasing birefringence was due to alignment of domains, not increased molecular order. Since their flow cell is three-dimensional with strong shear in the third dimension, the birefringence, measured along an optical path through the third dimension, relaxes downstream to a higher value than that far upstream. This effect does not exist in the simulations, and S relaxes toward the equilibrium value on the centerline. Given that our theoretical model does not contain distortional elasticity and our flow is two-dimensional, the agreement with experiments may seem surprising. A plausible explanation is that the contraction flow produces a rather homogeneous LCP configuration in which distortional elasticity is relatively unimportant. For similar reasons, the director alignment and order enhancement predicted here for the converging channel are qualitatively similar to predictions by Armstrong *et al.*,[24] who used a *nontumbling* version of the Doi theory.

In injection molded parts, the ''skin layer'' near the walls is usually well aligned.[42] This is caused by a combination of the fountain flow effect and the high shear rate at the wall. It is in the center of the channel that the LCP orientation is not easily controlled and defects abound. A contraction flow suppresses tumbling and induces a highly aligned state in just that region. This is a hopeful sign for the development of effective strategies for control of tumbling and disclinations in injection molding.

B. Abrupt contractions

For an abrupt contraction, the flow kinematics near the centerline is qualitatively the same as that for a gradual contraction. The main feature is an extensional region sandwiched by two rotational regions (Fig. 9). However, a new feature is the development of a corner vortex. Its size is somewhat larger than the Stokes flow vortex, but the vortex enhancement is much weaker than that typical of flexible polymers.[34] In terms of maximizing streamwise alignment and orientational order in the extensional flow region at the center of the channel, the abrupt contraction is found to be more effective than a gradual one with the same contraction ratio. Figure 10 compares a 1:0.5 sudden contraction with the 1:0.5 gradual contraction of Fig. 5. The stronger 1:0.25 sudden contraction is also shown. The abrupt contraction causes

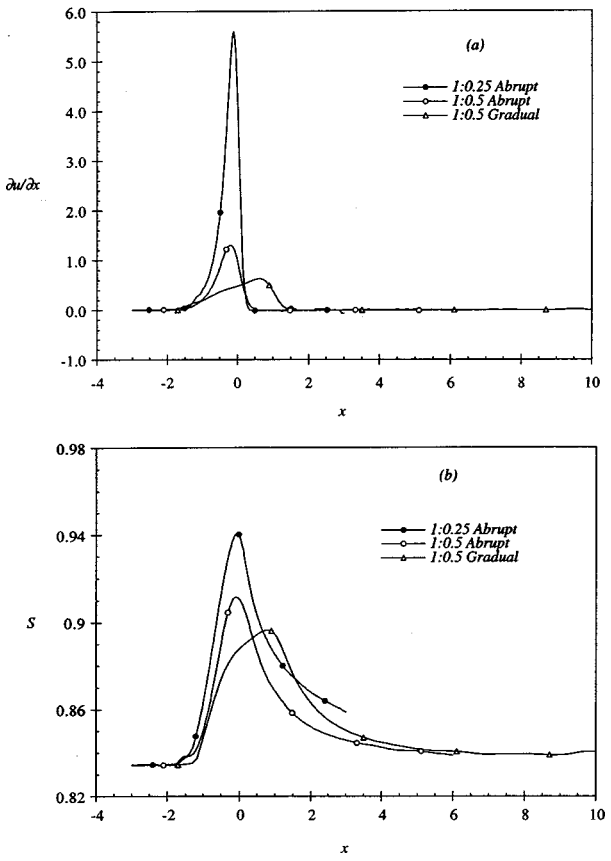

FIG. 10. Comparison between the 1:0.25 and 1:0.5 sudden contractions and the 1:0.5 gradual contraction. $t=50$. (a) The extension rate $\partial u/\partial x$ on the centerline; (b) the order parameter S on the centerline. For the 1:0.5 sudden contraction, the inlet is at $x=-3$ and the outlet is at $x=6$.

a stronger but shorter extensional flow and a higher degree of orientational order than the gradual contraction. The 1:0.25 contraction is even stronger and covers more or less the same length as the 1:0.5 sudden contraction. These predictions agree with qualitative observations of Bedford and Burghardt.[4]

As a practical means of improving polymer orientation, however, a gradual contraction is probably preferable to an abrupt one since the former produces a relatively uniform orientation and high order over a wider region, and also avoids the corner vortex, which is a source of disclinations. Director tumbling is induced by the rotational flow in the center of the vortex. Since the rotation is spatially inhomogeneous, the director field is distorted and disclination cores of $\pm 1/2$ strength are generated (Fig. 11). A $-1/2$ defect stays at the upper left-hand corner of the recirculating area and another at the lower right-hand corner. In the center of the vortex, defects of $\pm 1/2$ strength move as if convected by the flow; they interact and annihilate while new defects are continually created. The scenario is similar to that in an eccentric cylinder flow that we studied earlier.[22] It is important to note that distortional elasticity is neglected in the current model and symmetry of the director orientation is imposed about the flow plane. In a real LCP, the generation and subsequent evolution of disclinations probably contain additional physics.

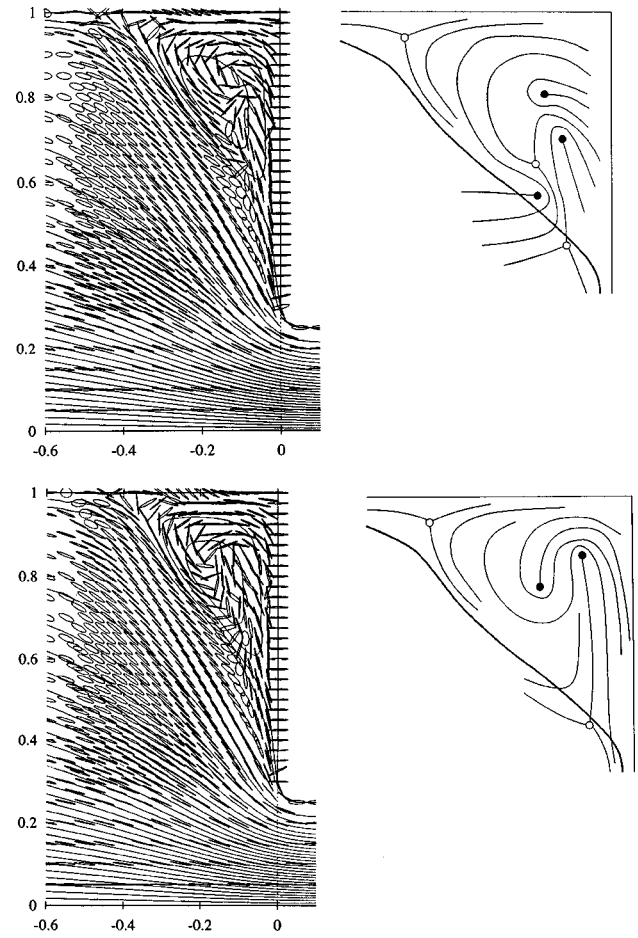

FIG. 11. Disclinations in the corner vortex. (a) $t=34$; (b) $t=46$. The sketches show the director lines in the corner, open and closed circles indicating $-1/2$ and $+1/2$ defects cores, respectively. The thick curve represents a streamline. There is a $-1/2$ defect at the upper left-hand corner of the recirculating area and another at the lower right-hand corner. In the center of the vortex, defects of $\pm 1/2$ strength are generated and annihilated continually.

V. EXPANSIONS

A. Gradual expansion

We have also computed the flow in a channel with a 0.5:1 gradual expansion. The geometry is the reverse of that in Fig. 5, except that now the inlet is at $x=-6$ and the outlet at $x=8$. Subject to a weak flow modification by the polymer, streamlines and flow-type parameter contours are also a reverse of those in Fig. 5. This reversal, of course, completely changes the deformation history and hence the polymer dynamics.

Figure 12 illustrates the dynamics of the LCP in this flow field. As in Fig. 7, we can divide the flow domain roughly into four areas. In the narrow channel upstream of the expansion, the polymer again behaves as in a straight channel, with director tumbling near the centerline. Within the expansion, director wagging is found in the near-wall region B with a frequency that decreases in the flow direction.

The effect of the expansion is most notable in the region near the centerline (area C). The expansion generates a compressive flow, and as may be expected, this tends to turn the

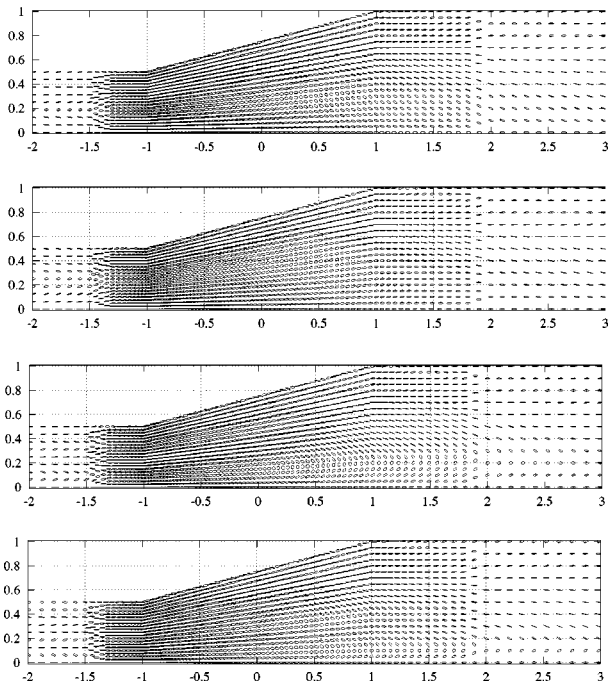

FIG. 12. The **A** field in the 0.5:1 gradual expansion at different times. (a) $t=24$. Four regions A–D are delineated based on the local polymer dynamics; (b) $t=28$; (c) $t=30$; note the tumbling layer above the centerline that starts at about $x=0$ and extends downstream. (d) $t=32.5$. The tumbling layer propagates toward the centerline as in Fig. 3.

director orthogonal to the streamlines. What is perhaps not so obvious is that the orientational order is also strongly reduced. Furthermore, unlike the contraction flow, the extensional flow due to the channel expansion *does not* fully suppress periodic motions of the director. Large amplitude wagging occurs in the upstream part of area C. Tumbling starts at $x\approx 0$ and extends downstream into the wide channel. This onset of tumbling near $x\approx 0$ may seem counter-intuitive because the flow is extensional immediately upstream of this area. However, the principal axis of extension in this compression flow is orthogonal to the flow direction, and the resultant rotation of the director away from the flow direction produces an increase in the amplitude of wagging, rather than a decrease as in the contraction flow. This increased amplitude eventually results in tumbling at $x\approx 0$. Downstream of the expansion (area D), wagging and tumbling occur in the near-wall and near-centerline parts of the wide channel, respectively.

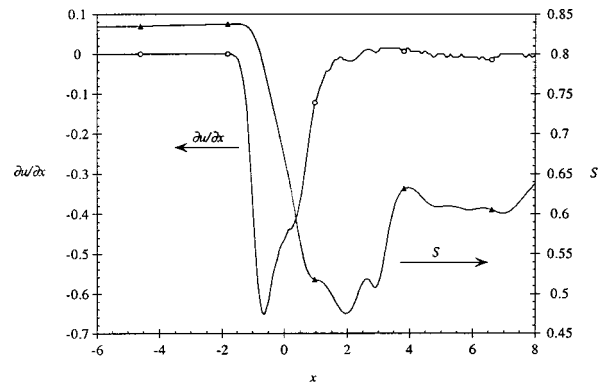

FIG. 13. The compression rate ($\partial u/\partial x$) and order parameter profiles along the centerline in the 0.5:1 gradual expansion, $t=30$.

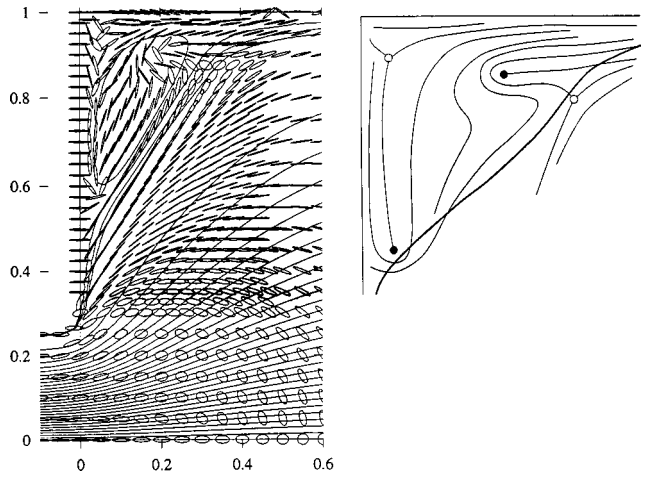

FIG. 14. The corner vortex and two pairs of disclinations in the 0.25:1 abrupt expansion at $t=33.62$. The corner at the lip of the expansion has been rounded to avoid stress singularity. Open and closed circles indicates $-1/2$ and $+1/2$ defects cores in the sketch. The thick curve represents a streamline.

Figure 13 shows the reduction in S along the centerline because of the compression. The fluctuations in the flow and the order parameter downstream of the expansion are similar to those in Fig. 8 but more prominent. These are results of flow modifications due to director wagging and tumbling in the wide channel. The spatial variation of the polymer stress changes the flow and that in turn affects **A**. Thus, even in the absence of distortional elasticity, director tumbling and wagging *off* the centerline can affect the order parameter *on* the centerline through flow modification.

Experimentally, Baleo and Navard[5] and Bedford and Burghardt[4] both found that an expansion reduces flow birefringence. While a contraction creates a region of relatively uniform and steady orientation and high order, an expansion of the same strength, measured by the strain rate, is not able to maintain an area of uniform and steady orientation (see Fig. 2 of Baleo and Navard[5]). These observations are consistent with our numerical results. In fact, area C in Fig. 12(a), where director wagging and tumbling occur, can be likened to zone II of Baleo and Navard[5] following a gradual expansion. Wang *et al.*[26] used a nontumbling Doi model to simulate the extrusion of LCP. Though they could not detect the tendency toward director wagging or tumbling following an expansion, they observed reduction in S and tilt of the director away from the streamline. These are consistent with our results.

B. Abrupt expansion

Finally, we consider a channel with a 0.25:1 sudden expansion at $x=0$; the inlet is at $x=-3$ and the outlet at $x=8$. The kinematics is similar to the 1:0.25 sudden contraction in Sec. IV B except that the deformation history is sampled backward by the polymer. There are two interesting areas in this flow. One is the corner vortex that contains

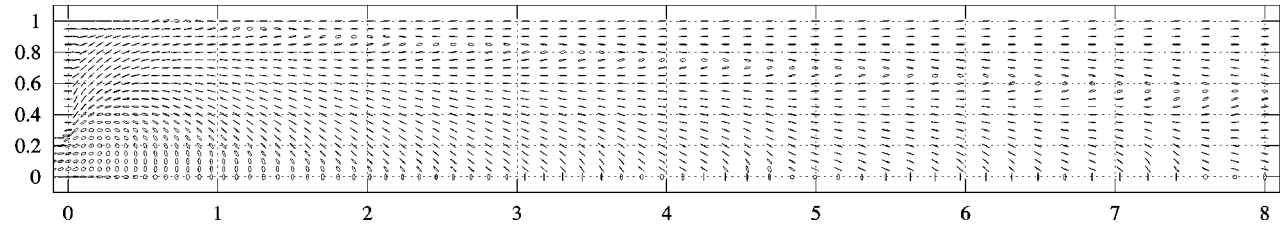

FIG. 15. The **A** field in the 0.25:1 abrupt expansion at $t=8.02$. On the centerline, the director is vertical and the order parameter, as indicated by the shape of the ellipses, varies periodically. Above the centerline there is a wave pattern in the orientation angle which extends to $y\approx 0.5$.

rotational flow. Disclination cores are generated as inhomogeneous tumbling distorts the director field. Figure 14 is a snapshot of the corner vortex. There are two pairs of half-strength defects and they will rotate and interact with one another. Positive and negative defects annihilate each other and new ones are created as in Fig. 11.

The other interesting area is the wide channel downstream of the expansion. A large-scale wave pattern develops and propagates downstream; the waves are roughly periodic temporally and also spatially along x. Figure 15 shows the configuration tensor **A** field at $t=8.02$. Because of the compression associated with the expansion, the ellipses are squeezed on the centerline; the director turns vertical and the order parameter becomes rather large. After the compression region ends at about $x=1$ (cf. contours of flow-type parameter in Fig. 9), one would expect the order parameter to relax gradually to the equilibrium value. In reality, however, the order parameter oscillates downstream with little relaxation; this gives rise to the cyclic ''squeeze-stretch'' pattern of the ellipses on the centerline.

The **A** field above the centerline also exhibits a wave pattern, although there it is the orientation angle θ that is readily seen to oscillate between large and small negative values. Figure 16 plots profiles of θ and the horizontal velocity component u along x at different elevations. Based on these and other numerical results, the following observations can be made.

(i) The $\theta(x)$ profiles show a wavy pattern that is synchronized with the S wave on the centerline. The $\theta(x)$ waves are phase locked at different y until about $y=0.5$. Above that the usual wagging behavior prevails.

(ii) The $u(x)$ profiles also show a wavy pattern with the same wave number as the θ waves.

(iii) By plotting such profiles at different times, we find that the S wave on the centerline and the θ and u waves off the centerline all travel with the mean centerline velocity, which is unity in this case, regardless of y and the local fluid velocity.

(iv) When the flow rate is doubled in the simulation, the wave number does not change and the onset of the waves stays roughly at the same position $x\approx 2$.

(v) Once in every few periods, the wave is distorted as near $x=5.5$ in Fig. 16. This modulation is probably an effect of the upstream wagging or tumbling that is not entirely eliminated by the expansion.

These waves bear remarkable similarity to an instability observed experimentally in channel flows following expansions.[4–6,40] That instability manifests itself as large-scale waves across the central part of the channel. The waves travel downstream at the centerline velocity. With increasing flow rate, the onset of the instability stays in the same position for HPC solutions[6] but moves upstream toward the expansion for PBG solutions.[40] The wave number is independent of the flow rate for both solutions. Bedford *et al.*[6] concluded that ''the wavy textures apparently emerge as a result of an inhomogeneous transition of orientation back to the flow direction, trapping thin bands of fluid in the twisted configuration.'' Considering that their ''twist'' refers to orientation orthogonal to the flow brought about by the expansion, this statement is an apt description of our Fig. 16(a). Since the experimental and simulated waves share these pe-

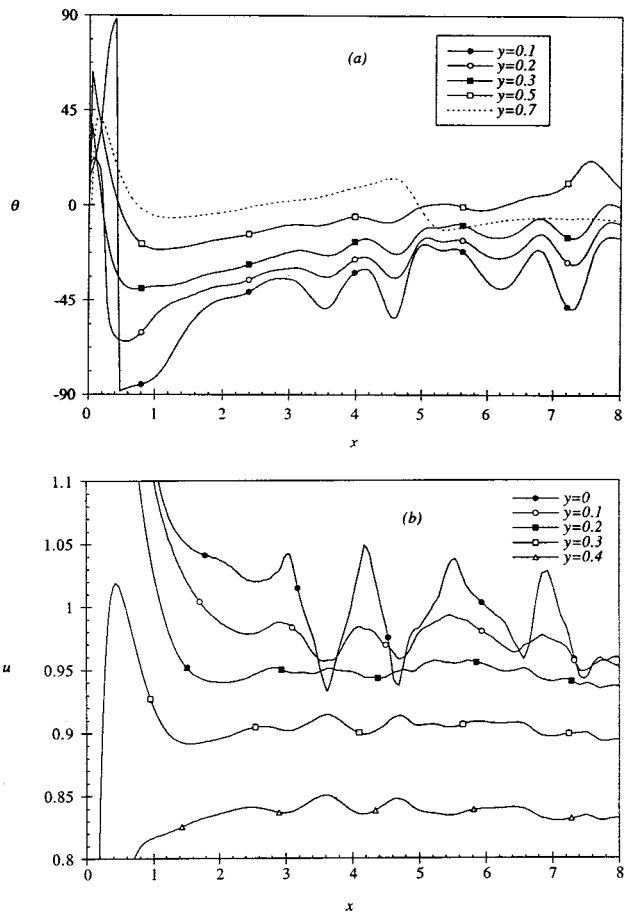

FIG. 16. The orientation angle profiles $\theta(x)$ and velocity profiles $u(x)$ at different y following the 0.25:1 sudden expansion. $t=8.02$. (a) The wavy pattern in θ persists to $y\approx 0.5$. At $y=0.7$ the usual wagging prevails. (b) The wavy pattern in u. The oscillation is strongest on the centerline and reverses phase at $y\approx 0.2$.

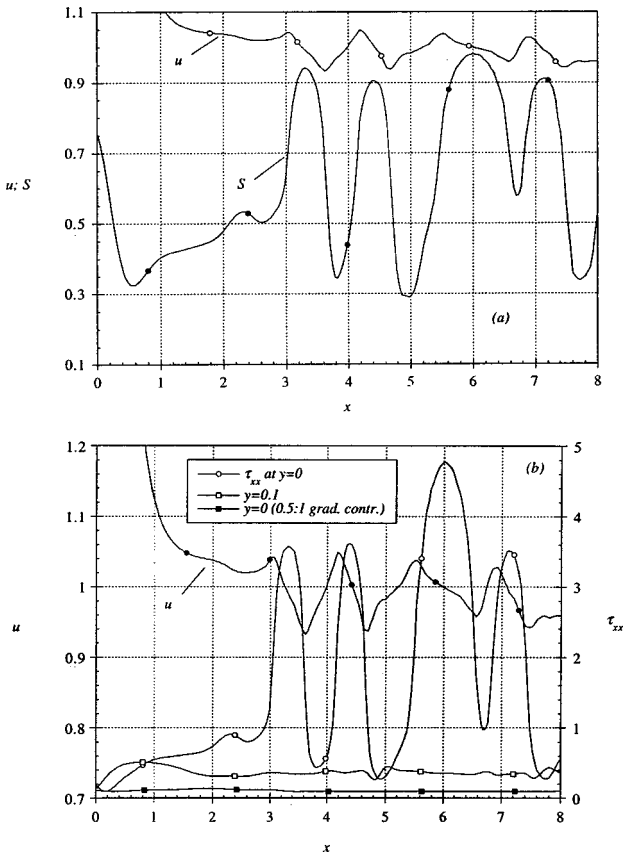

FIG. 17. The reinforcing disturbances on the centerline as the cause for the wavy pattern downstream of the 0.25:1 sudden expansion. $t=8.02$. (a) Fluctuations in u produces fluctuations in S through stretching and squeezing. (b) Through the normal stress, the polymer configuration in turn reinforces fluctuations in the velocity. Normal stress profiles at $y=0.1$ for the 0.25:1 sudden expansion and at $y=0$ for the 0.5:1 gradual expansion (at $t=30$) are also shown for comparison.

culiar features, one is tempted to assume that the two are of the same origin. Next we will first seek an explanation for the simulated waves and then see how that may apply to the experiments.

Because of the phase locking of the waves at different y, they must not be caused by the inherent wagging and tumbling tendencies since the time scale for such motion scales as the reciprocal of the local shear rate and thus varies with y. We propose that *the waves are an instability caused by the coupling between the fluid flow and polymer dynamics on the centerline*. Fig. 17(a) compares the $S(x)$ and $u(x)$ profiles on the centerline. The oscillation in S appears to be a consequence of the oscillating u; the maxima of S occur where the fluid is being squeezed ($\partial u/\partial x<0$) and the minima of S occur where the fluid is stretched ($\partial u/\partial x>0$). Therefore, if there is an initial disturbance in $u(x)$, it will cause a disturbance in $S(x)$ through the gradient $\partial u/\partial x$. This grows into an instability because the disturbance in $S(x)$ in turn reinforces the $u(x)$ disturbance through the polymer stress. On the centerline, the equation of motion for the fluid is

$$\mathrm{Re}\frac{\partial u}{\partial t}=-\frac{\partial p}{\partial x}+\frac{\partial^2 u}{\partial x^2}+\frac{c}{\mathrm{Pe}}\frac{\partial \tau_{xx}}{\partial x}. \tag{8}$$

With small inertia, τ_{xx} modifies the flow mainly through the viscous term; this can be seen as a stress balance:

$$\frac{\partial u}{\partial x}\approx-\frac{c}{\mathrm{Pe}}\tau_{xx}+p+\text{const.} \tag{9}$$

Figure 17(b) plots the polymer normal stress $\tau_{xx}(x)$ against $u(x)$. The downward slopes of u correspond to positive disturbances in τ_{xx} and so the magnitude of the compression rate will grow according to Eq. (9). By the same token, the upward slopes of u are enhanced by the negative disturbances in τ_{xx} and the extension rate will also grow. Hence the disturbances of u and S will reinforce each other on the centerline and an instability results. S is bounded by unity and rotary diffusion prevents perfect alignment of LCP molecules. Note that the fluid particles convect with more or less the wave speed and so they basically ride along on the waves. The small deviation of $u(x)$ from the wave speed implies that the fluid particles slide slowly on the slopes of the u wave. At any rate the polymer has ample time to sample the local deformation.

The most intriguing feature of Fig. 16 is that the wavy pattern persists well off the centerline. Owing to mass conservation, the squeezing–stretching on the centerline causes oscillation of the velocity field across the entire channel. This is effected by pumping the fluid toward the wall where the centerline is squeezed and toward the centerline where the centerline is stretched. Thus, there is a layer above $y=0$ in which the longitudinal velocity u varies in phase with the centerline velocity; above this layer, u varies *opposite* in phase to the centerline velocity. From Fig. 16(b), this layer exists in $y\leqslant 0.2$. Obviously, it cannot be the streamwise extension $\partial u/\partial x$ that causes the waves in $\theta(x)$ beyond $y=0.2$: $u(x)$ reverses phase at $y=0.2$ but $\theta(x)$ keeps the same phase through $y=0.5$.

The key to this puzzle is that the flow is two-dimensional away from the centerline. A disturbance in $\mathbf{v}$ affects the polymer configuration $\mathbf{A}$ through two components $\partial u/\partial x$ and $\partial v/\partial x$; the shear component $\partial u/\partial y$ probably has little to do with the waves since their frequency does not scale with the local shear rate. Though $v\ll u$, their gradients along x are comparable in magnitude. Results show that the oscillations of $\partial v/\partial x$ along x are phase locked throughout the channel, and these oscillations do correlate with the θ waves. An upward slope of $v(x)$ represents a ''counterclockwise'' shear and that corresponds to a θ maximum. Conversely downward slopes of $v(x)$ correspond to θ minima. Hence, the instability on the centerline, as depicted in Fig. 17, generates waves beyond the centerline by means of cross flow. This explains why the waves propagate downstream *with the centerline velocity*. Away from the centerline the influence of the polymer stress on the flow is secondary; the normal stress profile at $y=0.1$ in Fig. 17(b) illustrates how rapidly τ_{xx} diminishes away from the centerline. It should be noted that at $y>0$, the fluid particle slides backward on the wave forms of Fig. 16. This does not compromise the explanation of the θ waves by $\partial v/\partial x$ since the most recent deformation has the greatest effect on the LCP configuration.

Approaching the top wall, the velocity disturbances diminish and the natural tendency of director wagging quells the instability. This natural tendency can be discerned even closer to the centerline, for instance, in the gradual return of θ to the shear direction in Fig. 16(a). On the centerline, the instability shows no signs of sagging downstream (Fig. 17).

The final question about the simulated wave is why it does not occur following contractions and the 0.5:1 gradual expansion. The answer is that a strong expansion is needed to turn the director to vertical on the centerline such that the order parameter reacts to the stretching and squeezing in the way shown in Fig. 17(a); this reaction sets up the polymer stress that in turn reinforces the velocity disturbance. For the 0.5:1 gradual expansion, the director remains horizontal on the centerline. The polymer normal stress τ_{xx} is much smaller than that in the 0.25:1 sudden expansion [Fig. 17(b)], and the slight fluctuation downstream is caused by director tumbling and wagging off the centerline (cf. Fig. 13).

Now how relevant is the above explanation to the experimentally observed instability? The simulation differs from the experiments in two major aspects. First, the flow is three dimensional in the experiments, due not so much to roll cells as to the slit-flow geometry. The top and bottom walls, separated by a small gap, impose shearing orthogonal to the flow plane containing the expansion. Second, the theoretical model does not account for distortional elasticity and polydomains. Nonetheless, there are indications that the simulated and experimental waves may have the same origin in the flow-polymer coupling mechanism that we have proposed. Baleo and Navard[10] surmised that the expansion turns the director away from the streamline and that may lead to the instability. Based on quantitative data, Bedford *et al.*[6] further established the relationship between the director orientation at the expansion and the instability downstream. An ingenious ''twisted optical model'' represents the upstream orientational structure well. In addition, both Baleo and Navard[5] and Bedford and Burghard[4] found that a subsequent contraction in the channel removes the instability, presumably by realigning the director to the flow direction. Bedford *et al.*[6] also demonstrated that the instability is confined to the midplane of the slit flow where there is little complication from the orthogonal shear.

A definitive test of our proposal is the correlation between velocity and birefringence disturbances on the centerline of the channel. Bedford *et al.*[6] confirmed oscillations in the birefringence, though the amplitude is smaller than in Fig. 17. LDV measurements of the centerline velocity turned out rather random fluctuations, from which no signature of the wavy pattern could be found. As the authors remarked, ''given the inevitable coupling between liquid crystal orientation, rheological properties and velocity fields, one must assume that at some level the structural waves do influence the velocity field.'' Hence the lack of correlation may be due to limitations of LDV instrumentation. Note that the amplitude of velocity oscillation in Fig. 16(b) is only about 5% of the mean. As the measured oscillation in birefringence is much smaller than that in Fig. 17(a), the actual velocity fluctuation may be even smaller than 5%. The amplitude of velocity fluctuation in Fig. 10 of Ref. 6 is more than 5% of the mean. This issue unresolved, it is impossible to test the idea that the centerline communicates with the rest of the channel through cross flow. In particular, the experimental channels are rather wide and the velocity is essentially flat in the central region on the midplane. Thus, the cross-flow mechanism may be unnecessary for the synchronization of the wave across the width of the channel.

The experimental waves have three mysterious features that cannot be explained based on our simulations. The first is the strong dependence of the wave number on the thickness of the channel (cf. Fig. 7 of Bedford *et al.*[6]). Since the wave number is independent of the flow rate, and there is no shear on the midplane in any event, the orthogonal shear cannot be the answer. Since the Ericksen number is high, and the flow is definitely in a polydomain regime, it cannot be distortional elasticity originating from director anchoring at the solid walls. The Reynolds number in the experiments is estimated at 0.02, so fluid inertia cannot be responsible for the gap-width dependence, either. The second mystery is the narrow centerline disturbance that occurs for HPC solutions but not PBG solutions, and the third mystery is the sensitivity of the onset point to flow rate for PBG but not for HPC. The key to the last two puzzles is probably related to the differing flexibility of the molecules. Donald and Windle[43] listed the persistent length of both polymers. HPC has a shorter persistence length but a somewhat larger persistence ratio than PBG. It is interesting that our simulations, based on the Doi theory for thin and rigid rods, have shown no dependence of the onset position on the flow-rate.

VI. CONCLUSIONS

This paper is an attempt at simulating channel flows of LCPs while preserving the time-periodic nature of the polymer dynamics. Two simplifications are made: the distortional elasticity is neglected, and the flow is two-dimensional with director orientation symmetric about the flow plane. The main results of this paper can be summarized as follows.

(i) A contraction aligns the director with the streamline and improves the order parameter. The effects are stronger for larger contraction ratio. With the same contraction ratio, an abrupt contraction has stronger effects than a gradual contraction.

(ii) An expansion turns the director away from the flow direction and reduces the order parameter. As compared with a contraction having the same velocity gradient on the centerline, an expansion is ineffective in suppressing director wagging or tumbling and maintaining a relatively uniform director field.

(iii) If an expansion is strong enough to turn the director vertical on the centerline, an instability develops downstream because disturbances to the flow and polymer configuration reinforce each other through the polymer stress. This instability generates a wave that spans roughly the central half of the channel and propagates downstream at the centerline velocity.

(iv) Downstream of either an expansion or a contraction, the order parameter relaxes and director tumbling or wagging resumes.

(v) For abrupt contractions or expansions, disclinations of $\pm 1/2$ strength arise in the corner vortex. They rotate and annihilate each other periodically; new disclinations are generated continually.

Despite the simplifications in the theoretical model, most of the above results enjoy experimental support. For contraction flows this is perhaps expected since the extensional flow aligns the domains and makes distortional elasticity unimportant. The simulated instability is remarkably similar to experimental observations. Our explanation via the flow-polymer coupling mechanism is consistent with the clues that the experimenters have gathered, but the theory cannot be definitively validated by existing data.

The simulations indicate that using contraction/expansion is a feasible strategy for controlling LCP order and morphology in injection molding and extrusion. Contractions effectively suppress director tumbling in the center of the channel, precisely where ordering aid is needed. Expansions are problematic because they are less effective in controlling the motion of the director and are conductive to flow-structural instability. However, experiments show that a contraction following an expansion removes the instability. Since an expansion is less potent than a contraction in changing the LCP orientation and morphology, an expansion–contraction pair may achieve good ordering without constraining the dimensions of the product. Similarly, multiple contractions and expansions may be useful in designing channel flows.

ACKNOWLEDGMENTS

This research was supported by grants from the Fluid Dynamics program of the National Science Foundation and by the Materials Research Laboratory at UCSB. The computation was done at the NSF Supercomputer Centers in San Diego and Pittsburgh.

[1] R. G. Larson and D. W. Mead, ''The Ericksen number and Deborah number cascades in sheared polymeric nematics,'' Liq. Cryst. **15**, 151 (1993).
[2] N. Grizzuti, S. Guido, V. Nastri, and G. Marrucci, ''Velocity profiles in rectangular channel flow of liquid crystalline polymer solutions,'' Rheol. Acta **30**, 71 (1991).
[3] S. Guido, P. Frallicciardi, N. Grizzuti, and G. Marrucci, ''Rheo-optics of hydroxypropyl-cellulose solutions in Poiseuille flow,'' Rheol. Acta **33**, 22 (1994).
[4] B. D. Bedford and W. R. Burghardt, ''Molecular orientation of a liquid-crystalline polymer solution in mixed shear-extensional flow,'' J. Rheol. **40**, 235 (1996).
[5] J.-N. Baleo and P. Navard, ''Rheo-optics of liquid crystalline polymers in complex geometries,'' J. Rheol. **38**, 1641 (1994).
[6] B. D. Bedford, D. K. Cinader, and W. R. Burghardt, ''Unstable slit flow of a liquid crystalline polymer solution,'' Rheol. Acta **36**, 384 (1997).
[7] M. Kawaguchi and M. M. Denn, ''Visualization of the flow of a thermotropic liquid crystalline polymer in a tube with a conical contraction,'' J. Non-Newtonian Fluid Mech. **69**, 207 (1997).
[8] R. G. Larson, ''Roll-cell instabilities in shearing flows of nematic polymers,'' J. Rheol. **37**, 175 (1993).
[9] R. G. Larson and M. Doi, ''Mesoscopic domain theory for textured liquid crystalline polymers,'' J. Rheol. **35**, 539 (1991).
[10] B. J. Edwards, A. N. Beris, and M. Grmela, ''Generalized constitutive equation for polymeric liquid crystals. 1. Model formulation using the Hamiltonian (Poisson bracket) formulation,'' J. Non-Newtonian Fluid Mech. **35**, 51 (1990).
[11] Y. Farhoudi and A. D. Rey, ''Shear flows of nematic polymers. I. Orienting modes, bifurcations, and steady state rheological predictions,'' J. Rheol. **37**, 289 (1993).
[12] T. Tsuji and A. D. Rey, ''Effect of long range order on sheared liquid crystalline materials. I. Compatibility between tumbling behavior and fixed anchoring,'' J. Non-Newtonian Fluid Mech. **73**, 127 (1997).
[13] P. G. de Gennes, ''Phenomenology of short-range-order effects in the isotropic phase of nematic materials,'' Phys. Lett. A **30**, 454 (1969).
[14] J. Katriel, G. F. Kventsel, G. R. Luckhurst, and T. J. Sluckin, ''Free energies in the Landau and molecular field approaches,'' Liq. Cryst. **1**, 337 (1986).
[15] N. C. Andrews, B. J. Edwards, and A. J. McHugh, ''Continuum dynamics behavior of homogeneous liquid-crystalline polymers under the imposition of shear and magnetic fields,'' J. Rheol. **39**, 1161 (1995).
[16] F. Greco, ''Field equation of nematostatics,'' Mol. Cryst. Liq. Cryst. **290**, 139 (1996).
[17] M. Doi, ''Molecular dynamics and rheological properties of concentrated solutions of rodlike polymers in isotropic and liquid crystalline phases,'' J. Polym. Sci., Polym. Phys. Ed. **19**, 229 (1981).
[18] M. Doi and S. F. Edwards, *The Theory of Polymer Dynamics* (Oxford University Press, London, 1986).
[19] R. G. Larson, ''Arrested tumbling in shear flows of liquid crystalline polymers,'' Macromolecules **23**, 3983 (1990).
[20] J. J. Magda, S.-G. Baek, K. L. DeVries, and R. G. Larson, ''Shear flows of liquid crystal polymers: Measurements of the second normal stress difference and the Doi molecular theory,'' Macromolecules **24**, 4460 (1991).
[21] G. Marrucci and F. Greco, ''Flow behavior of liquid crystalline polymers,'' Adv. Chem. Phys. **86**, 331 (1993).
[22] J. Feng and L. G. Leal, ''Simulating complex flows of liquid crystalline polymers using the Doi theory,'' J. Rheol. **41**, 1317 (1997).
[23] G. Marrucci and P. L. Maffettone, ''Nematic phase of rodlike polymers. II. Polydomain predictions in the tumbling regime,'' J. Rheol. **34**, 1231 (1990).
[24] R. C. Armstrong, S. Ramalingam, and D. E. Bornside, ''A finite-element model to predict structure development in spinneret flow of liquid-crystalline polymers,'' Proceedings SPE ANTEC, 1995, p. 2590.
[25] N. Mori, Y. Tsuji, K. Nakamura, and C. Yoshikawa, ''Numerical simulations of the flow of liquid crystalline polymers between parallel plates containing a cylinder,'' J. Non-Newtonian Fluid Mech. **56**, 85 (1995).
[26] H. Wang, R. C. Armstrong, and R. A. Brown, ''A finite-element model to predict structure development in extrusion of liquid-crystalline polymers,'' Proceedings of the 12th International Congress on Rheology, 1996, pp. 167–168.
[27] G. Marrucci and F. Greco, ''The elastic constants of Maier–Saupe rodlike molecule nematics,'' Mol. Cryst. Liq. Cryst. **206**, 17 (1991).
[28] F. Greco and G. Marrucci, ''Molecular structure of the hedgehog point defect in nematics,'' Mol. Cryst. Liq. Cryst. **210**, 129 (1992).
[29] C. V. Chaubal and L. G. Leal, ''A closure approximation for liquid crystalline polymer models based on parametric density estimation,'' J. Rheol. **42**, 177 (1998).
[30] C. V. Chaubal, L. G. Leal, and G. H. Fredrickson, ''A comparison of closure approximations for the Doi theory of LCPs,'' J. Rheol. **39**, 73 (1995).
[31] J. Feng, C. V. Chaubal, and L. G. Leal, ''Closure approximations for the Doi theory: Which to use in simulating complex flows of LCPs,'' J. Rheol. **42**, 1095 (1998).
[32] M. van Gurp, ''On the use of spherical tensors and the maximum entropy method to obtain closure for anisotropic liquids,'' J. Rheol. **42**, 1269 (1998).
[33] Consider the flow to be unidirectional (along x) at the exit. Momentum balance in the transverse y direction gives: $p(y)=p_0+\tau_{yy}$, p_0 being the pressure at the center of the channel where $\tau_{yy}=0$. Then the surface traction along x is: $f_x=-p+\tau_{xx}=-p_0+(\tau_{xx}-\tau_{yy})$ and does not vanish for all y at the exit.
[34] B. Purnode and M. J. Crochet, ''Flows of polymer solutions through contractions. 1. Flow of polyacrylamide solutions through planar contractions,'' J. Non-Newtonian Fluid Mech. **65**, 269 (1996).
[35] P. M. Gresho and R. L. Sani, ''On pressure boundary conditions for the incompressible Navier–Stokes equations,'' in *Finite Elements in Fluids*, edited by R. H. Gallagher, R. Glowinski, P. M. Gresho, J. T. Oden, and O. C. Zienkiewicz (Wiley, New York, 1987), Vol. 77, Chap. 7.
[36] O. Pironneau, ''Conditions aux limites sur la pression pour les équations de Stokes et de Navier–Stokes,'' C. R. Acad. Sci., Ser. I: Math. **303**, 403 (1986).

[37]D. Doraiswamy and A. B. Metzner, ''The rheology of polymeric liquid crystals,'' Rheol. Acta **25**, 580 (1986).
[38]R. G. Larson and H. C. Öttinger, ''Effect of molecular elasticity on out-of-plane orientation in shearing flows of liquid crystalline polymers,'' Macromolecules **24**, 6270 (1991).
[39]G. Marrucci, ''Tumbling regime of liquid-crystalline polymers,'' Macromolecules **24**, 4176 (1992).
[40]B. D. Bedford and W. R. Burghardt, ''Molecular orientation and instability in plane Poiseuille flow of a liquid crystalline polymer,'' J. Rheol. **38**, 1657 (1994).
[41]The flow-type parameter indicates the relative strength of the extensional and rotational components of the flow. For a purely extensional flow, a simple shear and a purely rotational flow, $\lambda=1$, 0, and -1, respectively. For the definition of λ, see P. Singh and L. G. Leal, ''Finite-element simulation of the start-up problem for a viscoelastic fluid in an eccentric rotating cylinder geometry using a third-order upwind scheme,'' Theor. Comput. Fluid Dyn. **5**, 107 (1993).
[42]Z. Ophir and Y. Ide, ''Injection molding of thermotropic liquid crystal polymers,'' Polym. Eng. Sci. **23**, 792 (1983).
[43]A. M. Donald and A. H. Windle, *Liquid Crystalline Polymers* (Cambridge University Press, Cambridge, 1992).